interaction with surfactants.

Conclusion

The present work shows that copolymers of 1-pyreneacrylic acid with methacrylic acid and acrylic acid show significant structural changes with pH, structural changes that affect the pyrene environment. The changes may be interpreted in terms of what is already known from NMR, light scattering, and other physical measurements with regard to PMA unwinding with increasing pH. This lends support to the present studies on insights that can be gained from photophysical studies of probes, either solubilized or bound to polymer systems. In particular, the location of the probe molecule, either at the chain end, randomly bound to the chain, or simply solubilized in compact PMA, indicates different stages of opening of the polymer as its degree of dissociation increases. In each case a discrete pH region is indicated. However, the uncoiling of PMA appears to be a continuous process over several pH units. The present studies show that the fluorescent probe pyrene is a sensitive indicator of the conformational behavior of PMA. Water-soluble polymers are often used as solubilizing or stabilizing agents for many colloidal systems such as clays, where the polymer may bind to the clay edge and prevent flocculation. Little is known about the nature of this binding, but copolymers containing fluorescent probes could give useful information on the nature of the polymer colloid binding, e.g., on the environment of colloidal clay edges.

Registry No. $TlNO_3$, 10102-45-1; $CuSO_4$, 7758-98-7; O_2, 7782-44-7; NaI, 7681-82-5; CPC, 123-03-5; (1-pyreneacrylic acid)·(methacrylic acid) (copolymer), 91816-90-9; (1-pyreneacrylic acid)·(acrylic acid) (copolymer), 91816-91-0; pyrene, 129-00-0; poly(methacrylic acid), 25087-26-7; nitromethane, 75-52-5.

References and Notes

(1) We thank the National Science Foundation for support of this work via Grant CHE 82-01226.
(2) Turro, N.; Grätzel, M.; Braun, A. *Angew. Chem.* **1980**, *19*, 675.
(3) Fendler, J. "Membrane Mimetic Chemistry"; Academic Press: New York, 1983.
(4) Thomas, J. K. *Chem. Rev.* **1980**, *80*, 283.
(5) Geacintov, N. E.; Prusik, T.; Khosrofian, J. *J. Am. Chem. Soc.* **1976**, *98*, 6444.
(6) Nosaka, Y.; Kira, A.; Imamura, M. *J. Phys. Chem.* **1981**, *85*, 1353.
(7) Barone, G.; Crescenzi, V.; Quadrifoglio, F. *J. Phys. Chem.* **1967**, *71*, 2341.
(8) Chen, T.; Thomas, J. K. *J. Polym. Sci., Part A-1* **1979**, *17*, 1103.
(9) Ermolenko, I. N.; Katibnikov, M. A. *Vysokomol. Soedin.* **1962**, *4*, 1249. Tan, K. L.; Treloar, F. E. *Chem. Phys. Lett.* **1980**, *73*, 234 and references therein. Meisel, D.; Rabani, J.; Meyerstein, D.; Matheson, M. S. *J. Phys. Chem.* **1978**, *82*, 985. Jonah, C. D.; Matheson, M. S.; Meisel, D. *Ibid.* **1979**, *83*, 257. Taha, I. A.; Morawetz, H. *J. Polym. Sci., Part A-2* **1971**, *9*, 1669. Taha, I. A.; Morawetz, H. *J. Am. Chem. Soc.* **1971**, *93*, 829.
(10) Strauss, U. P.; Vesnaver, G. *J. Phys. Chem.* **1975**, *79*, 1558. Strauss, U. P.; Schlesinger, M. S. *J. Phys. Chem.* **1978**, *82*, 1627.
(11) DellaGuardia, R.; Thomas, J. K. *J. Phys. Chem.* **1983**, *87*, 990.
(12) Katchalsky, A.; Eisenberg, H. *J. Polym. Sci.* **1951**, *6*, 145.
(13) Silberberg, A.; Eliassaf, J.; Katchalsky, A. *J. Polym. Sci.* **1957**, *23*, 259.
(14) Okamoto, H.; Wada, Y. *J. Polym. Sci., Part A-2* **1974**, *12*, 2413.
(15) Kay, P. J.; Kelly, D. P.; Milgate, G. I.; Treloar, F. E. *Makromol. Chem.* **1976**, *177*, 885.

Monte Carlo Calculations of Particle Scattering Functions of Polymer Chains

C. J. C. Edwards†

Department of Polymer Science and Technology, University of Manchester Institute of Science and Technology (UMIST), Manchester M60 1QD, U.K., and Department of Pure and Applied Chemistry, Strathclyde University, Glasgow G1 1XL, U.K.

R. W. Richards

Department of Pure and Applied Chemistry, Strathclyde University, Glasgow G1 1XL, U.K.

R. F. T. Stepto*

Department of Polymer Science and Technology, University of Manchester Institute of Science and Technology (UMIST), Manchester M60 1QD, U.K.

Received November 23, 1982

ABSTRACT: Relationships between particle scattering functions and chain structure are investigated through calculations of $P(Q)$ for unperturbed polymethylene (PM), poly(oxyethylene) (POE), and poly(dimethylsiloxane) (PDMS) chains of up to 150 skeletal bonds. The calculations employ a Monte Carlo technique with Metropolis sampling and realistic rotational isomeric state models (RISM) using established molecular parameters. $P(Q)$ is calculated for each accepted configuration of a Metropolis sample using the exact Debye expression for a collection of point scatterers. For PM and POE, scattering centers are assumed to be located in the chain backbone, and for PDMS the effect of offsetting the scattering centers to account for the methyl side groups is investigated. Differences in contrast factors between chain segments and background medium, which are important for comparisons with experimental data, are also taken into account and are shown to affect the form of $P(Q)$ in the intermediate-Q and high-Q regimes. A moment expansion method used previously in the literature is investigated for PM and shown, except for $Q < 0.1$ Å^{-1}, to give values of $P(Q)$ in poor agreement with those from the full, Monte Carlo procedure. The effects of chain length, chain structure, and flexibility (temperature) on the form of $P(Q)$ are illustrated and discussed.

Introduction

Small-angle neutron scattering (SANS)[1-4] allows measurements of the scattered intensity from polymeric systems to be made over a much wider range of scattering vector Q ($=(4\pi/\lambda)\sin(\theta/2)$) than is accessible using classical light scattering.[5] Experimentally

$$I(Q)/I(0) = P(Q)S(Q) \quad (1)$$

when $I(Q)$ and $I(0)$ denote the scattered intensity at Q =

† Present address: Unilever Research Port Sunlight Laboratory, Bebington, Wirral, Merseyside L63 3JW, U.K.

0024-9297/84/2217-2147$01.50/0

Q and $Q = 0$, respectively. $P(Q)$ is the particle scattering factor which characterizes scattering from individual molecules and $S(Q)$ is a structure factor associated with the presence of intermolecular correlations. In dilute solution, $S(Q) \cong 1$ and $I(Q)/I(0) \simeq P(Q)$. In this paper, the discussion is confined to the particle scattering factor $P(Q)$ and so the results are applicable to dilute solutions and systems for which $S(Q)$ is known.

Both $P(Q)$ and $S(Q)$ are related by Fourier transforms to appropriate pair distribution functions of distances between scattering centers. The particle scattering function for a system of x point scatterers can be written as[6]

$$P(Q) = \frac{1}{x^2}\sum_i^x\sum_j^x \langle \exp(i\mathbf{Q}\cdot\mathbf{r}_{ij})\rangle \tag{2}$$

when $\mathbf{r}_{ij}$ is the vector connecting scattering centers i and j. On averaging over all orientations eq 2 reduces to[6]

$$P(Q) = \frac{1}{x^2}\sum_i^x\sum_j^x \left\langle \frac{\sin(Qr_{ij})}{Qr_{ij}} \right\rangle \tag{3}$$

For molecules containing scattering centers of unequal scattering power, or contrast, eq 3 can be generalized to give

$$P(Q) = \sum_i^x\sum_j^x \frac{g_i g_j \left\langle \frac{\sin(Qr_{ij})}{Qr_{ij}} \right\rangle}{\sum_i^x\sum_j^x g_i g_j} \tag{4}$$

where g_i and g_j are the contrast factors for segments i and j, respectively. At low Q, in the so-called Guinier regime ($Q\langle s^2\rangle^{1/2} \ll 1$), eq 3 further simplifies to

$$P(Q) = 1 - \frac{Q^2\langle s^2\rangle}{3} \tag{5}$$

where $\langle s^2\rangle$ is the mean-square radius of gyration of the molecule.

For a collection of identical point scatterers with a single Gaussian probability density for end-to-end vectors of subchains (the Gaussian subchain model), Debye[7] derived the following expression for $P(Q)$

$$P(Q) = \frac{1}{(Q^2\langle s^2\rangle)^2}(Q^2\langle s^2\rangle - 1 + e^{-Q^2\langle s^2\rangle}) \tag{6}$$

It is well-known that eq 6 does not adequately represent the form of $P(Q)$ at high Q ($Q\langle s^2\rangle^{1/2} \gg 1$) for many unperturbed polymers. Polymers with complex architectures such as branched or cyclic species and chains which are perturbed by excluded volume effects deviate even more markedly from eq 6.

Neutrons are scattered by interactions with atomic nuclei, and to calculate $P(Q)$ exactly, the double sums in eq 4 should be evaluated for all pairs of nuclei in the molecule using the appropriate values of g_i and g_j. This would mean that for most polymers the calculation of $P(Q)$ would be prohibitively time-consuming. However, approximations can be introduced to make the problem more tractable. For instance, nuclei which are attached to the same skeletal atom (e.g., the atoms in a $-CH_2-$ repeat unit) can be approximated as point scatterers located on the skeletal atoms. This will give the correct form of $P(Q)$ at low Q, when large distances are dominant, but may lead to errors at high Q. Yoon and Flory[8] have shown that SANS data[9] for short polymethylene (PM) chains in the range $0.2 \lesssim Q \lesssim 0.4$ Å^{-1} can only be exactly reproduced by evaluating the double sums in eq 3 over all protons in the chains. Recently, Hayashi, Flory, and Wignall[10] have extended this work to polyisobutylene (PIB) chains of relatively high molar mass and obtained excellent agreement between theory and experiment. However, valuable information about the general form of $P(Q)$ for particular polymers and variations with chain length and temperature can be obtained by treating scattering centers as being located on or near to skeletal atoms in the polymer chain. The ability to predict the form of $P(Q)$ in the intermediate-Q range from a detailed knowledge of chain structure using eq 4 offers the possibility of extracting more information from a scattering experiment than simply the radius of gyration.

Previous calculations of $P(Q)$ for unperturbed polymer chains have been reviewed recently.[11] Heine et al.[12] used a Monte Carlo technique and a persistence chain model to evaluate $P(Q)$ for chains with varying degrees of stiffness. Their results agree qualitatively with measured scattering functions, but the persistence chain model takes little account of the detailed chain structure and its usefulness may be limited.

Flory et al.[13-15] adopted a different approach for unperturbed chains using the RISM and realistic molecular parameters and the Nagai series expansion of the function $\sin(Qr_{ij})/Qr_{ij}$. The scattering centers are approximated as being segments in the chain backbone, although attempts have also been made to account for scattering centers in pendant side groups. $\sin(Qr_{ij})/Qr_{ij}$ can be expanded in even moments $\langle r_{ij}^{2p}\rangle$ of r_{ij} and for sufficiently long chains $\langle r_{ij}^{2p}\rangle$ can be replaced by $\langle r_n^{2p}\rangle$. In other words, $\langle r_{ij}^{2p}\rangle$ becomes insensitive to the position of i and j in the chain and can be replaced by the $2p$th moment of the end separation of a chain of n bonds, where $n = |i - j|$. The even moments of r for a chain of n bonds can easily be calculated using generator matrix techniques[16] and the upper limits to p and n are governed by the available computer time. To avoid matrix calculations of moments of higher orders,[14,15] results from the Nagai series were supplemented by Monte Carlo evaluations of $\sum\sum\langle\sin(Qr_{ij})/Qr_{ij}\rangle$ for selected smaller values of $|i - j|$. It has been shown previously[17,18] that the Nagai series is oscillatory and converges slowly. Calculations of $P(Q)$ for an unperturbed PM chain of 100 skeletal bonds, using the Nagai series approach, are presented in the next section and further illustrate the limitations of this method. However, it should be noted that the oscillations in $P(Q)$ for syndiotactic PMMA are apparently well reproduced by use of the Nagai series.[15]

Recently, a development[19-21] of the generator matrix method of Flory et al.[13-15] has been proposed to treat perturbed chains. However, the method of Flory can only be applied in a self-consistent manner to unperturbed chains. In general, calculations of $P(Q)$ for excluded volume chains and chains of finite length require the numerical evaluation of $P(Q)$ through eq 4 and realistic chain models. Since complete enumeration techniques can only be used for very short chains, Monte Carlo calculations are required to evaluate $P(Q)$ for polymeric chains.

Previous Monte Carlo calculations of $P(Q)$ for polymer chains have been reported.[8,10,17] Zierenberg, Carpenter, and Hsieh[17] (ZCH) used a Monte Carlo method with randomly generated samples and eq 3 to calculate $P(Q)$ for PM chains and compared their results with $P(Q)$ given by the Nagai series expansion. However, they replaced r_{ij} in eq 3 by r_{1j} (in other words they assumed r_{ij} to be independent of the position of i in the chain). The error resulting from this assumption is discussed in the next section. As mentioned previously, Yoon and Flory[8] calculated $P(Q)$ for short PM chains using a Monte Carlo technique and compared their results with experimental SANS data ob-

tained by Dettenmaier for n-C_{16} and n-C_{36} chains. They showed that the experimental data at high Q could only be reproduced by taking the protons as scattering centers.

More recently, Hayashi, Flory, and Wignall[10] have devised a Monte Carlo method, which can take explicit account of all scattering nuclei in the chain, to calculate $P(Q)$ for unperturbed polyisobutylene (PIB) chains of 800 monomer units. Excellent agreement is obtained with both SANS and X-ray scattering measurements over a wide range of Q values. The method uses conditional probabilities applicable to unperturbed chains to compile a histogram of distances between all pairs of scattering centers in the molecular and evaluates $P(Q)$ from the histogram.

In this paper we assume that scattering centers are located on or near skeletal atoms and the general effects of chain length and temperature are investigated. A Monte Carlo technique based on Metropolis sampling[22,23] is employed, which has been used previously to investigate the configurational statistics of isolated linear and cyclic chains,[24-26] of chains adsorbed onto a surface,[27,28] diffusion coefficients,[29,30] and $P(Q)$ for linear and cyclic PDMS,[31] including a fitting of experimental data. The Metropolis algorithm has the advantage that calculated quantities converge to their equilibrium values in a well-characterized manner and can be applied to both perturbed and unperturbed chains. The use of large sample sizes ensures that the uncertainty in $P(Q)$ is less than 1%. Hence, in the present paper smooth curves are drawn through the calculated points.

Particle scattering functions, $P(Q)$, have been calculated for unperturbed PM, poly(oxyethylene) (POE), and linear poly(dimethylsiloxane) (PDMS) chains containing up to 150 skeletal bonds, using eq 4 and the aforesaid Monte Carlo technique. The polymers have increasingly complicated chain structures from the relatively simple PM chain with one type of chain segment to PDMS with two types and widely differing bond angles and large methyl side groups. Scattering functions have been calculated up to $Q = 1.0$ Å^{-1}, although for neutron scattering experiments the incoherent background generally becomes dominant for $Q \gtrsim 0.5$ Å^{-1}. The calculations on PM were carried out in order to examine the usefulness of the Nagai series, the behavior of real chains relative to the Gaussian subchain model as a function of chain length and flexibility, and to provide a comparative basis for interpreting the predicted behavior of POE and PDMS. The effect of varying the relative magnitudes of the contrast factors g_i and g_j, to model experimental conditions by taking account of different solvent backgrounds, is investigated for POE and PDMS. The scattering centers are usually positioned on the atoms in the chain backbone, although for PDMS the effect of including offset scattering centers is investigated.

Computational Technique

A rotational isomeric state model (RISM) chain of x segments is generated and its configurational energy (which may include both local and nonlocal contributions) is calculated. In this paper, nonlocal interactions between segments are suppressed and the chains are effectively unperturbed by excluded volume effects. The configuration of the chain is changed by randomly altering the rotational states of typically three contiguous skeletal bonds, and the new energy and the energy difference $\Delta E = E_{new} - E_{old}$ are computed. If ΔE is negative the new configuration is accepted and the running averages of the properties of interest are computed. For $\Delta E > 0$ the new configuration is accepted with probability $\exp(-\Delta E/kT)$, and if the configuration is rejected the properties of the old configuration are counted into the sample again. For large sample sizes (typically 10^5 configurations for $x = 100$) this procedure leads to a Boltzmann ensemble of chains.

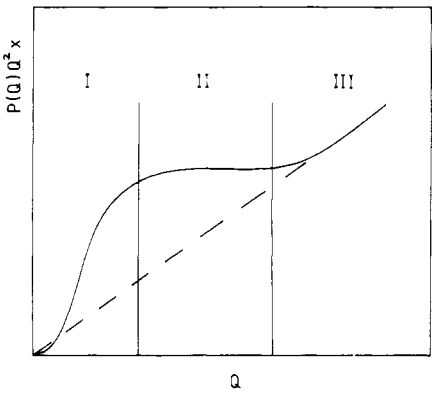

Figure 1. Schematic Kratky plot ($P(Q)Q^2x$ vs. (Q) for a "typical" polymer chain. (I) Guinier regime (slope → 0 as $Q \to 0$). (II) Plateau region. (III) Linear behavior at high Q, extrapolating linearly back to the origin.

For present purposes values of $\sin(Qr_{ij})/Qr_{ij}$ are generated for all i and j, and $P(Q)$ is evaluated by using eq 4. For chains with two types of scattering centers, the contrast ratio is given by the equation

$$\frac{g_i}{g_j} = \frac{(\rho_i - \rho_m)^2}{(\rho_j - \rho_m)^2} \tag{7}$$

where $\rho = (\sum b/v)$ is the scattering length density of a segment with total scattering length $\sum b$ and volume v. Values of v are calculated from experimental densities and van der Waals radii. Values of b are tabulated elsewhere for the commonly occurring nuclei which make up the scattering centers considered here.[2] ρ_m, the scattering length density of the background medium, is calculated in the same manner and for $\rho_m = 0$ the chain is effectively in vacuo, a situation which cannot be attained experimentally. For a homopolymer with identical scattering centers, eq 3 is employed to calculate $P(Q)$.

Results and Discussion

Calculated values of $P(Q)$ can conveniently be presented with the so-called Kratky plot[11] of $P(Q)Q^2x$ vs. Q. A schematic Kratky plot is shown in Figure 1 and three different regions can be identified. At low Q, when $Q\langle s^2\rangle^{1/2} \ll 1$, the radius of gyration of the polymer molecule can be obtained from $P(Q)$ through eq 5. In the intermediate-Q regime, scattering from segments separated by relatively short distances in the molecule becomes dominant and the scattered intensity can reach an asymptotic limit given, for the Gaussian subchain model, by $P(Q)Q^2x \equiv 2xK^*c/\langle s^2\rangle$ (where c is the concentration and K^* is an experimental constant). At high Q there is a further upturn in the plot of $P(Q)Q^2x$ vs. Q which results from the effects of scattering from individual nuclei. Consequently the scattered intensity in this region would be expected to become independent of chain length as Q increases.

Polymethylene. The RISM of PM employed here was developed by Abe, Jernigan, and Flory[32] and has t, g^+, and g^- states situated at 0°, 112.5°, and −112.5°, respectively with rotational energies $E_\sigma = 400$ cal mol^{-1} and $E_\omega = 1500$ cal mol^{-1}. Scattering centers in the PM chain are taken as being centered on the skeletal carbon atoms. Figure 2 shows a Kratky plot for a PM chain of 100 skeletal bonds at 298 K, where $P(Q)$ has been calculated using the Nagai series expansion truncated at the 10th moment of r. The figure shows clearly that the Nagai series has not converged by the 10th moment and that the start of oscillatory be-

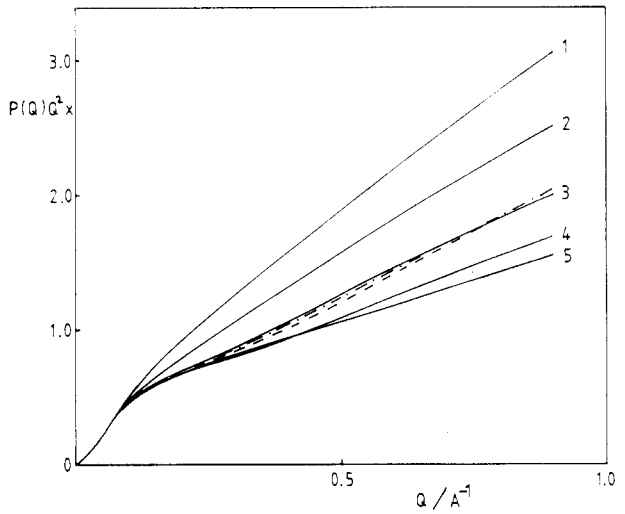

Figure 2. Kratky plots for an unperturbed PM chain with 101 skeletal atoms at 298 K: Nagai series expansion up to the $2p$th moment of r, for p = 1–5; (--) Monte Carlo calculation using eq 3; (-·-) Monte Carlo calculation using the ZCH approximation.

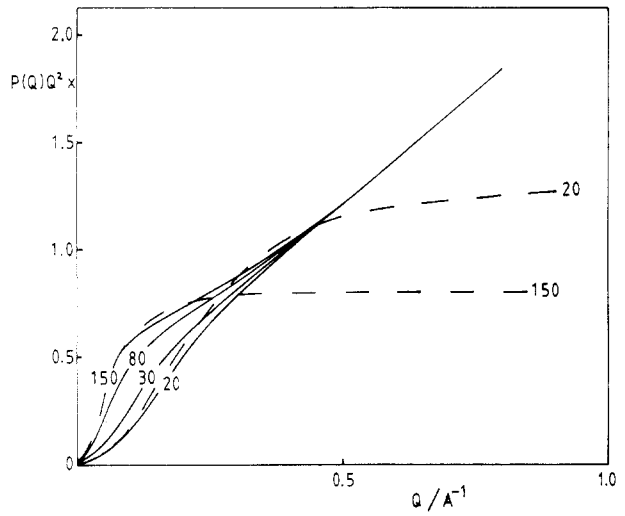

Figure 3. Kratky plots for unperturbed PM chains at 298 K as a function of chain length: (—) calculated using Monte Carlo method and eq 3 at chain lengths shown; (--) from eq 6. Numbers of skeletal atoms shown with curves.

havior is indicated. These observations are in keeping with previous results.[14,17,18] The dashed curve in Figure 2 represents the present Monte Carlo calculation of $P(Q)$ for a 100 skeletal bond PM chain using eq 3 in its full form. The Nagai series shows no sign of converging to this limit for $Q \gtrsim 0.1$ Å^{-1}. The dot-dashed curve represents the equivalent calculation but replacing r_{ij} by r_{1j} as reported previously by ZCH. The curve in the ZCH approximation lies closest to the 6th moment of the Nagai series expansion and overestimates $P(Q)$ by about 5% at intermediate Q compared to the full Monte Carlo calculation. The difference between the two dashed curves is not important and would be expected to diminish with increasing chain length. However, it is expected to become significant for perturbed chains due to the increased dependence of r_{ij} on the positions of i and j in the chain.

Figure 3 shows a Kratky plot for PM chains of various chain lengths at 298 K, for Q = 0 to Q = 1.0 Å^{-1}. Also shown are the appropriate Gaussian approximations to $P(Q)$, calculated with eq 6 and the radii of gyration of the chains in question. At low Q the agreement between the Monte Carlo technique and eq 6 is excellent, but there are large deviations at intermediate Q and high Q, reflecting

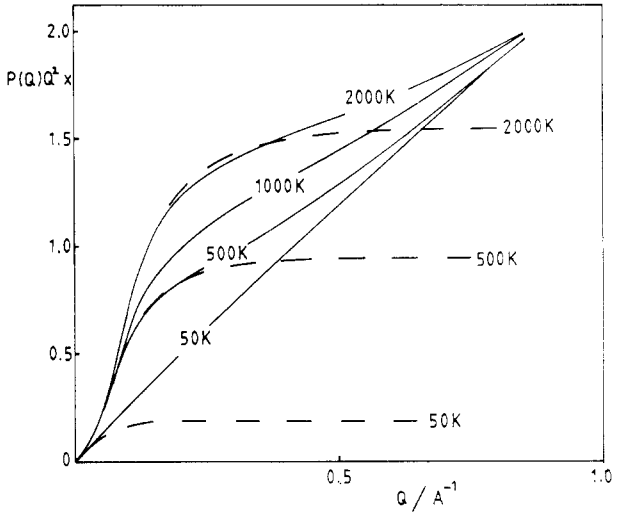

Figure 4. Kratky plots for unperturbed PM chain with 101 skeletal atoms as a function of temperature: (—) calculated using Monte Carlo method and eq 3 at temperatures shown; (--) from eq 6.

the non-Gaussian nature of the pair distribution functions of r_{ij} for small $|i - j|$. The Monte Carlo calculations produce an upturn in the Kratky plot at high Q, corresponding to that shown in Figure 1 and $P(Q)Q^2x$ becomes independent of chain length. The plateau region is compressed at the short lengths considered here.

Figure 4 shows a plot of $P(Q)Q^2x$ vs. Q for a PM chain of 101 skeletal atoms as a function of temperature as well as the Gaussian approximations to $P(Q)$ at three temperatures. At 50 K, when the contribution to the average configuration of the chain from the all-trans configuration becomes dominant, $P(Q)Q^2x$ approaches the linear rigid-rod limit, while at higher temperatures the plateau region of the Kratky plot starts to appear. However, agreement between the Monte Carlo calculations and the Gaussian approximation never becomes complete, again due to the effects of non-Gaussian distributions of r_{ij} for small $|i - j|$ becoming emphasized as Q increases.

Poly(oxyethylene). The RISM of POE used in these calculations has been described previously by Mark and Flory.[33] Since the POE chain contains both $-CH_2-$ and $-O-$ units, the ratio of contrast factors depends on the scattering length density of the background medium (ρ_m). Calculations have been performed for $g_i = g_j$, when the subscripts i and j denote $-O-$ and $-CH_2-$, respectively, as well as for hydrogenous POE in D_2O (g_i/g_j = 0.00133), H_2O (g_i/g_j = 30.6), and in vacuo (g_i/g_j = 417). Previous calculations by Yoon and Flory[14] employed the Nagai series method to calculate $P(Q)$, for $Q < 0.3$ Å^{-1}, and assumed that the scattering was centered on the oxygen atoms. This corresponds to the case of hydrogenous POE in H_2O, whereas SANS measurements have generally been carried out in D_2O.

Figure 5 shows a Kratky plot for POE chains of a variety of chain lengths in D_2O at 298 K. As for PM, $P(Q)Q^2x$ becomes independent of chain length of high Q, although the upturn in the Kratky plot is less marked and the plateau is more marked than for PM. Also shown in Figure 5 are the Gaussian approximations, using calculated values of $\langle s^2 \rangle$ and eq 6, to the scattering functions for POE chains with 19 and 148 segments. As for PM, the agreement between the Gaussian approximation and eq 4 is excellent at low Q, but there are significant deviations for $Q > 0.15$ Å^{-1}. The more marked plateau at intermediate Q appears to be due to the contrast factors employed rather than the configurational statistics of the chain. Subsidiary calcu-

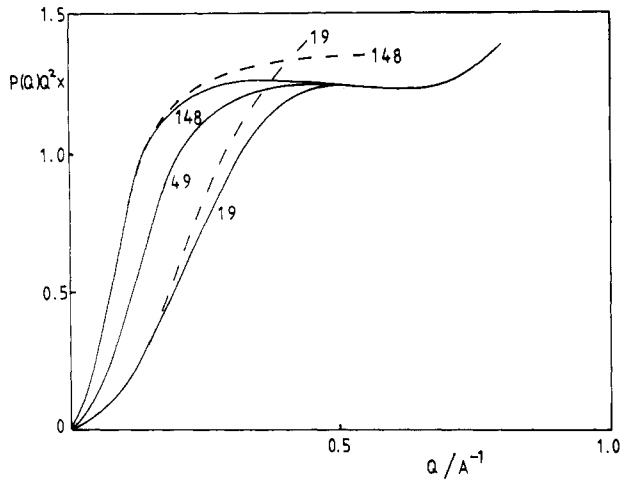

Figure 5. Kratky plots for unperturbed POE chains at 298 K with the numbers of skeletal atoms shown: $g_i/g_j = 0.0013$, when subscripts i and j denote –O– and $-CH_2-$, respectively; (—) calculated using Monte Carlo method and eq 4; (– –) from eq 6.

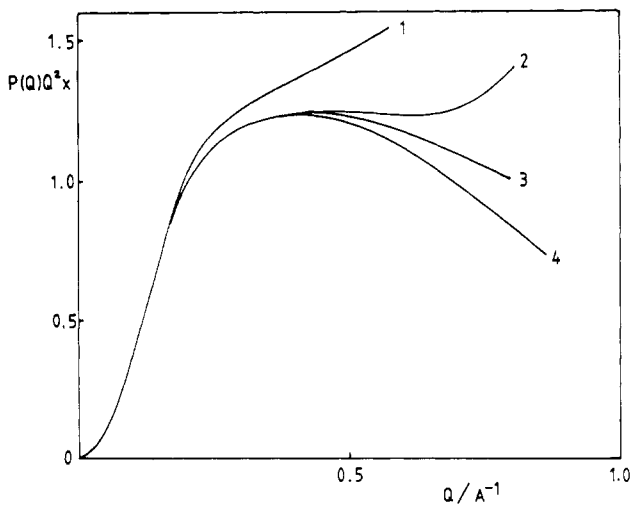

Figure 6. Kratky plots for POE with 100 skeletal atoms at 298 K, with different ratios of contrast factors: curve 1, $g_i = g_j$; curve 2, $g_i/g_j = 0.0013$ (POE/D_2O); curve 3, $g_i/g_j = 30.6$ (POE/H_2O); curve 4, $g_i/g_j = 417$ (POE in vacuo). ($i \equiv$ –O–, $j \equiv -CH_2-$).

lations for a PM chain with every third scattering center given zero weighting produce similar behavior to that shown in Figure 5 for POE. The change in behavior with contrast factor is further illustrated in Figure 6 where a Kratky plot is shown for a POE chain with 100 skeletal atoms and a range of contrast ratios g_i/g_j. Increased weighting of separations of the order of one bond length ($g_i = g_j$) produces an increase in $P(Q)Q^2x$ at high Q (curve 1) similar to that observed previously for PM. The previous calculations by Yoon and Flory[14] for POE did not extend to high enough Q to show this region of the Kratky plot.

Figure 7 illustrates the temperature dependence of the scattering function for a 100 skeletal atom POE chain in D_2O. In contrast to the case for PM where the chain tends to the all-trans rigid-rod configuration at low temperatures, the POE chain tends to a helical structure at low temperature. This apparently results in the characteristic maximum in the Kratky plot at intermediate Q, which increases in magnitude with decreasing temperature.

Poly(dimethylsiloxane). The detailed chain model of PDMS has been given previously by Flory, Crescenzi and Mark.[34] The PDMS chain consists of $-Si(CH_3)_2-$ and –O– units so that, as for POE, the ratio of contrast factors depends on the scattering-length density of the background

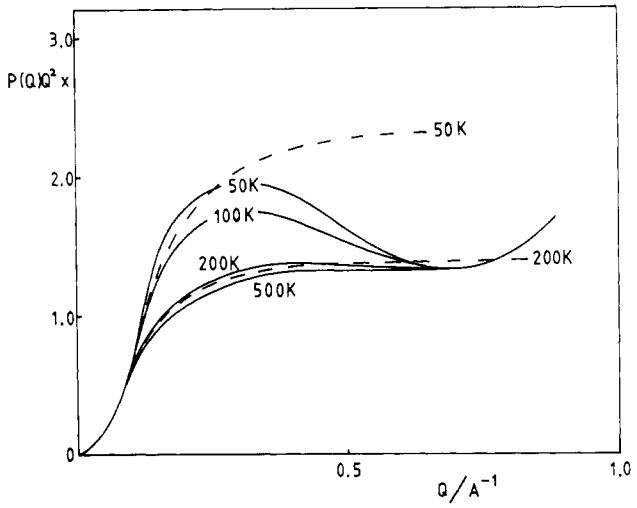

Figure 7. Kratky plots for POE with 100 skeletal atoms as a function of temperature: $g_i/g_j = 0.0013$ (POE/D_2O, $i \equiv$ –O–, $j \equiv -CH_2-$); (—) calculated using Monte Carlo method and eq 4; (– –) from eq 6.

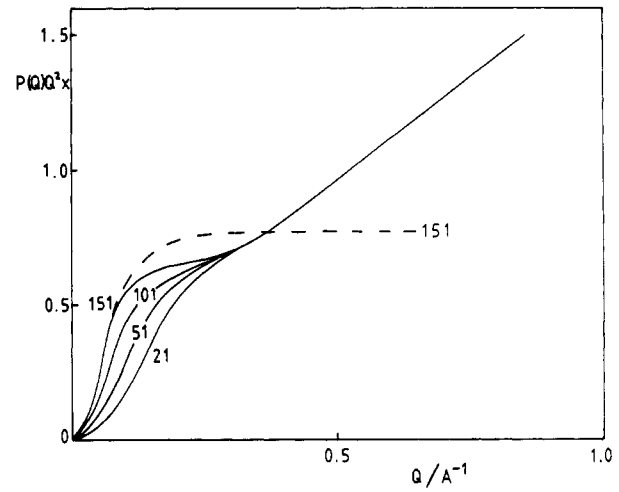

Figure 8. Kratky plots for PDMS chains with numbers of skeletal atoms shown at 298 K as a function of chain length: $g_i/g_j = 0.135$ (PDMS/C_6D_6), $i \equiv$ –O–, $j \equiv -Si(CH_3)_2-$; (—) calculated using Monte Carlo method and eq 4; (– –) from eq 6.

medium ρ_m. The cases considered here are $g_i = g_j$, where the subscripts i and j denote –O– and $-Si(CH_3)_2-$, respectively, and hydrogenous PDMS in deuteriobenzene C_6D_6 ($g_i/g_j = 0.135$), in C_6H_6 ($g_i/g_j = 1.3$), and in vacuo ($g_i/g_j = 44.6$).

Figure 8 shows a Kratky plot for PDMS of various chain lengths in C_6D_6 at 298 K with scattering from the $-Si(CH_3)_2-$ group centered on the skeletal silicon atom. The plots are similar to those obtained for PM with $P(Q)Q^2x$ becoming independent of chain length at high Q.

The effects of temperature are illustrated in Figure 9 for a 101 skeletal atom PDMS chain in C_6D_6. Decreasing temperature produces a maximum in the Kratky plot at $Q \cong 0.25$ Å^{-1}, which in fact corresponds to $u = Q\langle s^2\rangle^{1/2} \cong 2$ (as T and hence $\langle s^2\rangle^{1/2}$ decrease, the maximum shifts to slightly higher Q). As for POE, this is due to the predominance of helical sequences at low temperatures. However, the low-energy all-trans configuration of PDMS is planar and forms a closed ring for $x = 22$, which for the model unperturbed chain corresponds to a helix of zero pitch. In reality the trans torsional angle of the PDMS chain is probably slightly distorted at low temperatures to allow the formation of a helix with a suitable pitch, although this is not taken into account here. In this

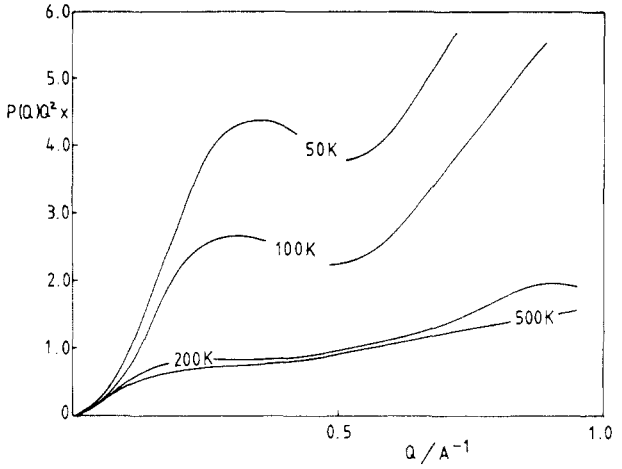

Figure 9. Kratky plots for PDMS chain with 101 skeletal atoms as a function of temperature: $g_i/g_j = 0.135$ (PDMS/C_6D_6, $i \equiv$ –O–, $j \equiv$ –Si$(CH_3)_2$–); (—) calculated using Monte Carlo method and eq 4.

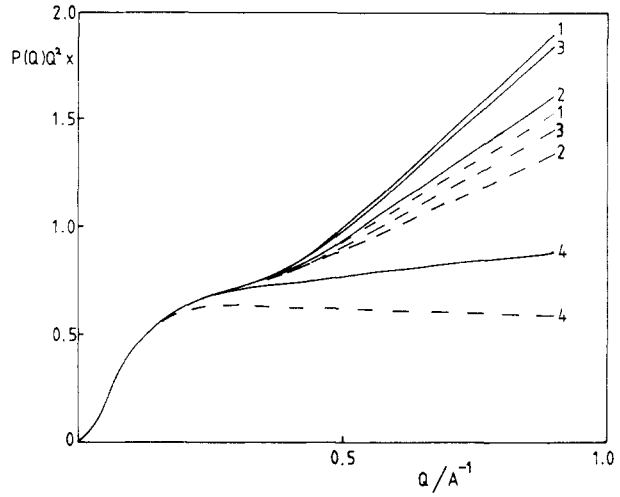

Figure 10. Kratky plots for PDMS chain with 101 skeletal atoms at 298 K with different ratios of contrast factors: (—) Scattering centered on skeletal atoms; (– –) offset scattering centers; curve 1, $g_i = g_j$; curve 2, $g_i/g_j = 0.135$ (PDMS/C_6D_6); curve 3, $g_i/g_j = 1.3$ (PDMS/C_6H_6); curve 4, $g_i/g_j = 44.6$ (PDMS in vacuo) ($i \equiv$ –O–, $j \equiv$ –Si$(CH_3)_2$–).

context the presence of a maximum in the Kratky plot for cyclic PDMS at 296 K and $u \cong 2$ has been observed experimentally[31] and predicted computationally[31] using the present Monte Carlo technique. In addition, the existence of a maximum at $u = 2.15$ has been predicted generally for cyclic polymers by Burchard and Schmidt[35] using the Gaussian subchain model.

The behavior of the curves for PDMS at high values of Q may be contrasted with those for PM (Figure 4) and POE (Figure 7). The latter two sets of curves each coalesce to give temperature-independent behavior over small distances. However, PDMS shows a temperature sensitivity over the whole range of values of Q investigated. Thus chain flexibility is affecting the number of scattering centers which are separated by distances down to a fraction of an Å. This contrasting behavior must be linked with the increased statistical weights of configurations composed of all-trans rings of 22 atoms, which produce helical sections in the chain with scattering centers from adjacent turns of the helix, being situated in close mutual proximity.

In Figure 10 the effects of varying the contrast ratio g_i/g_j are illustrated together with those of offsetting the –Si$(CH_3)_2$– scattering center. For PDMS, the total scattering lengths of a silicon atom and a methyl group are 0.42×10^{-12} and -0.457×10^{-12} cm, and the resulting difference in contrast means that the effective scattering center for the –Si$(CH_3)_2$– group will be considerably offset from the silicon atom. This can be approximately accounted for by storing an additional set of coordinates corresponding to the effective scattering center, which is the center with respect to contrast factors of the silicon atom and the two methyl groups. These scattering units form a triangle and the position of the effective scattering center can be calculated using the known values of g as weights in a "center of mass" type formula. Offsetting the effective scattering center reduces the scattered intensity, due to the increase in the shortest separation of scattering centers in the chain and can produce effects of similar magnitude to those found by varying the ratio of contrast factors. The effect of offsetting the scattering center extends to values of Q as low as 0.1 $Å^{-1}$. In this respect, the present result is in qualitative accord with the findings of Yoon and Flory for short PM chains[8] and Hayashi, Flory, and Wignall[10] for the unperturbed PIB chain.

Conclusions

A Monte Carlo technique, using Metropolis sampling, has been used to calculate $P(Q)$ for realistic RISM chains containing up to 150 skeletal bonds. The calculations employ the exact expression for $P(Q)$ for a system of point scatterers (eq 4) with scattering occurring at effective segmental centers. Calculations have been performed for PM, POE, and PDMS chains which are unperturbed by excluded volume effects. Realistic chain models have been used throughout the calculations and experimentally realizable values of g_i/g_j have been employed. The varied forms of Kratky plots obtained illustrate the importance of accounting for chain structure and experimental conditions (temperature and contrast factors) even at relatively low values of Q. The same Monte Carlo technique and PDMS RISM with non-offset –Si$(CH_3)_2$– scattering centers has already[31] been used to explain experimental SANS measurements of $P(Q)$ for cyclic and linear PDMS up to $u \simeq 4$.

For PM, it is shown that the replacement of r_{ij} in eq 2 by r_{1j} can lead to a slight overestimate of $P(Q)$ at intermediate Q for short chains where end effects are important. The Nagai series for $\sin(Qr_{ij})/Qr_{ij}$ is shown to be nonconvergent and oscillatory in keeping with the findings of previous workers.[14,17,18]

The ratio of contrast factors g_i/g_j is shown to be important in the calculation of $P(Q)$ at intermediate Q and high Q for chains with more than one type of scattering center. Reduction of the contribution to $P(Q)$ from pairs of scattering centers separated by only one or two skeletal bonds produces a reduction in $P(Q)$ at high Q. $P(Q)$ has also been calculated for PDMS chains with offset scattering centers to allow for the presence of methyl side groups on the silicon atoms of the chain. The effect of offsetting the silicon-based scattering centers is to reduce the scattered intensity and the effects are of the same order of magnitude as those produced by varying the ratio of contrast factors.

The effects of temperature variation have been investigated and the transition from a low-temperature rigid-rod (PM) or helix (POE and PDMS) to more freely rotating chains at high temperatures is clearly seen. Agreement with the Gaussian subchain approximation for $P(Q)$ (eq 6) is good in the Guinier regime in all cases; however, at higher Q the agreement is poor at all chain lengths at low temperatures, but improves with increasing temperature as expected. Irrespective of chain length, the agreement is never complete at intermediate Q and high Q, due to the

failure for small values $|i - j|$ of the assumption that the density distribution functions of r_{ij} follow a single Gaussian distribution for all i and j.

Acknowledgment. C.J.C.E. acknowledges the financial support of the Science and Engineering Research Council. We also thank D. Rigby for invaluable contributions to the original development of the Monte Carlo programs.

Registry No. PM (SRU), 25038-57-7; POE (SRU), 25322-68-3.

References and Notes

(1) Richards, R. W. In "Developments in Polymer Characterization"; Dawkins, J. V., Ed.; Applied Science Publishers: England, 1978.
(2) Maconnachie, A.; Richards, R. W. *Polymer* **1978**, *19*, 739.
(3) Ullmann, R., *Annu. Rev. Mater. Sci.* **1980**, *10*, 261.
(4) Higgins, J. S. In "Neutron Scattering and Materials Science"; Kostorz, G., Ed.; Academic Press: New York, 1978.
(5) Kratochvil, P. In "Light Scattering from Polymer Solutions"; Huglin, M., Ed.; Academic Press: London/New York, 1972; Chapter 7.
(6) Debye, P. *Ann. Phys. (Leipzig)* **1915**, *46*, 809.
(7) Debye, P. *J. Phys. Chem.* **1947**, *51*, 18.
(8) Yoon, D. Y.; Flory, P. J. *J. Chem. Phys.* **1978**, *69* (6), 2537.
(9) Dettenmaier, M. *J. Chem. Phys.* **1978**, *68* (5), 2319.
(10) Hayashi, H.; Flory, P. J.; Wignall, G. D. *Macromolecules* **1983**, *16*, 1328.
(11) Kirste, R. L.; Oberthur, R. L. In "Small-Angle X-ray Scattering"; Glatter, O., Kratky, O., Eds.; Academic Press: London, 1982.
(12) Heine, S.; Kratky, O.; Roppert, J. *Makromol. Chem.* **1962**, *56*, 150.
(13) Flory, P. J.; Jernigan, R. L. *J. Am. Chem. Soc.* **1968**, *90*, 3128.
(14) Yoon, D. Y.; Flory, P. J. *Macromolecules* **1976**, *9*, 294.
(15) Yoon, D. Y.; Flory, P. J. *Macromolecules* **1976**, *9*, 299.
(16) Flory, P. J. "Statistical Mechanics of Chain Molecules"; Interscience: New York, 1969.
(17) Zierenberg, B.; Carpenter, D. K.; Hsieh, J. H. *J. Polym. Sci., Polym. Symp.* **1976**, *54*, 145.
(18) Mattice, W. L.; Carpenter, D. K. *J. Chem. Phys.* **1976**, *64* (8), 3261.
(19) Mattice, W. L.; Santiago, G. *Macromolecules* **1980**, *13*, 1560.
(20) Mattice, W. L. *Macromolecules* **1982**, *15*, 18.
(21) Mattice, W. L. *Macromolecules* **1982**, *15*, 579.
(22) Wood, W. W. In "Physics of Simple Liquids"; Temperley, H. N. V., Rowlinson, J. S., Rushbrooke, G. S., Eds.; North-Holland Publishing Co.: Amsterdam, 1968; Chapter 5.
(23) Lal, M.; Spencer, D. "Applications of Computer Techniques in Chemical Research"; Hepple, P., Ed.; Applied Science Publishers: England, 1972.
(24) Winnik, M. A.; Rigby, D.; Stepto, R. F. T.; Lemaire, B. *Macromolecules* **1980**, *13*, 699.
(25) Edwards, C. J. C.; Rigby, D.; Stepto, R. F. T.; Dodgson, K.; Semlyen, J. A. *Polymer* **1983**, *24*, 391.
(26) Edwards, C. J. C.; Rigby, D.; Stepto, R. F. T.; Semlyen, J. A. *Polymer* **1983**, *24*, 395.
(27) Lal, M.; Stepto, R. F. T. *J. Polym. Sci., Polym. Symp.* **1977**, *61*, 401.
(28) Higuchi, A.; Rigby, D.; Stepto, R. F. T. "Adsorption in Solution"; Ottewill, R. H., Rochester, C. H., Smith, A. L., Eds.; Academic Press: New York, 1983.
(29) Mokrys, I. J.; Rigby, D.; Stepto, R. F. T. *Ber. Bunsenges. Phys. Chem.* **1979**, *83*, 446.
(30) Edwards, C. J. C.; Rigby, D.; Stepto, R. F. T. *Macromolecules* **1981**, *14*, 1808.
(31) Edwards, C. J. C.; Richards, R. W.; Stepto, R. F. T.; Dodgson, K.; Higgins, J. S.; Semlyen, J. A. *Polymer* **1984**, *25*, 365.
(32) Abe, A.; Jernigan, R. L.; Flory, P. J. *J. Am. Chem. Soc.* **1966**, *88*, 631.
(33) Mark, J. E.; Flory, P. J. *J. Am. Chem. Soc.* **1965**, *87*, 1415.
(34) Flory, P. J.; Crescenzi, V.; Mark, J. E. *J. Am. Chem. Soc.* **1964**, *86*, 146.
(35) Burchard, W.; Schmidt, M. *Polymer* **1980**, *21*, 745.

Theory of Helix–Coil Transitions of α-Helical, Two-Chain, Coiled Coils. Analytic Treatment of the Homopolymeric, Neglect-Loop-Entropy Model

Jeffrey Skolnick†

Department of Chemistry, Washington University, St. Louis, Missouri 63130.
Received September 23, 1983

ABSTRACT: Analytic expressions for the internal partition function and helix content in the limit of infinite molecular weight, f_{hd}^{∞}, are derived for homopolymeric, α-helical, two-chain, coiled coils (dimers) in which the effects of loop entropy and mismatch are neglected, i.e., the neglect-loop-entropy model. We examine the behavior of f_{hd}^{∞} as a function of the helix–helix interaction parameter, w, and as a function of the Zimm–Bragg helix initiation parameter, σ. Comparison is made between the helix–coil transition in infinite-length dimers and in an "analogous", isolated, single-chain, homopolypeptide. Furthermore, the dependence of the helix content of the dimer on chain length is investigated for various values of σ. On the basis of the present work, it is concluded that homopolypeptide dimers having the same degree of polymerization as the prototypical two-chain, coiled coil tropomyosin are in the short to moderate length limit, a necessary condition for the application of the theory that includes loop entropy and mismatch (*Macromolecules* **1984**, *17*, 645).

I. Introduction

In a series of papers, a statistical mechanical model of the helix–coil transition in two-chain, coiled coils (dimers) has been developed.[1-4] The theory ascribes to each individual amino acid two "short-range" interaction parameters, the standard Zimm–Bragg helix initiation parameter, σ, and helix propagation parameter s, that are assumed to depend only on amino acid types and not on amino acid sequence.[5] Furthermore, the theory accounts for the greatly increased helix content of the side-by-side, two-chain, coiled coil relative to the calculated helix content of isolated single chains by a "long-range" interaction parameter w; $-RT \ln w$ is the free energy of the positionally fixed interacting pair of helical turns in each of the two chains relative to the free energy of the positionally fixed pair of turns in the noninteracting chains. The theory has been extended to include the effects of loop entropy and mismatch on the helix–coil transition.[2-4] For a detailed account of the theory as well as a discussion of the relevant

† Alfred P. Sloan Foundation Fellow.

0024-9297/84/2217-2153$01.50/0